

Scavenging Wind Energy by Triboelectric Nanogenerators

Bo Chen, Ya Yang,* and Zhong Lin Wang*

To meet future needs for clean and sustainable energy, tremendous progress has been achieved in development for scavenging wind energy. The most classical approach is to use the electromagnetic effect based wind turbine with a diameter of larger than 50 m and a weight of larger than 50 ton, and each of them could cost more than \$0.5 M, which can only be installed in remote areas. Alternatively, triboelectric nanogenerators based on coupling of contact-electrification and electrostatic induction effects have been utilized to scavenge wind energy, which takes the advantages of high voltage, low cost, and small size. Here, the development of a wind-driven triboelectric nanogenerator by focusing on triboelectric materials optimization, structure improvement, and hybridization with other types of energy harvesting techniques is reviewed. Moreover, the major applications are summarized and the challenges that are needed to be addressed and development direction for scavenging wind energy in future are highlighted.

1. Introduction

In view of concerns about global climate change and energy crisis, developing new energy sources which are renewable and environment friendly is one of the most urgent challenges to the development of human society.^[1–4] Harvesting energy directly from surrounding environment can be a promising and effective solution to achieve the sustainability of our daily life.^[5–8] Wind energy, a clean and widespread type of mechanical energy, has attracted more and more attention and may play a significant role in electricity supply in future.^[9–11] Roughly 4.3% of globally electricity demand was realized by wind power technologies as of the end of 2015.^[12] However, as constrained by the extra-large size, high cost of installation, and geographical environment, wind power equipment can hardly be utilized in our daily living environment, such as in urban city areas.^[13–15] In this regard, it is essential to develop innovative strategies

and technologies to collect wind energy in living environment. Since the invention of triboelectric nanogenerator (TENG) in 2012, it was extensively investigated and showed lots of advantages including small scale, low cost, easy fabrication, and portability.^[16–22] Plenty of wasted mechanical energy in our daily life, such as vibration, human motion, wind, flowing water, and rotating tire, can be utilized by different TENG structures.^[23–27] The wind-driven triboelectric nanogenerator (WD-TENG), which is considered as an important tributary in TENG family, can also serve as self-powered sensors for actively monitoring wind speed, humidity, as well as breath-out alcohol concentration.^[28–30] Figure 1 illustrates the comparison between the conventional wind energy harvester (wind turbine) and the new wind energy harvester (WD-TENG) in terms of the mechanism, characteristics, as well as disadvantages.

Herein, this article first reviews typical triboelectric materials and structures for fabricating WD-TENG, which can significantly affect the output performance of WD-TENG. The outstanding output voltage and current of various WD-TENG can reach as high as 400 V (with a size of $22 \times 10 \times 67 \text{ mm}^3$) and 3.4 mA (with a radius of 70 mm), respectively.^[31,32] The output voltage and current can be adjusted through transformer and a power management circuit to satisfy different electrical equipment's demands. Hybridizing WD-TENG and other types of generators is more suitable to meet needs of varying environments.^[33–35] Moreover, the remarkable electrical performance endows WD-TENG lots of practical applications including powering electrical equipment, charging energy storage devices, as well as serving as self-powered sensors. As a new generation of sustainable, renewable, and green energy source, WD-TENG is expected to be widely used in human daily life in near future.

2. Fundamental Working Modes and Triboelectric Materials

Triboelectrification, also known as contact electrification, is a common phenomenon in people's life.^[36,37] It has been identified as a negative effect in some situations, like causing fire and dust explosion, whereas this effect exists almost everywhere. A promising strategy to utilize rather than reduce triboelectrification is to convert and stockpile it into other forms of energy. Despite triboelectrification could be generated by almost any material in daily life, it is still a serious challenge to collect and convert this tiny energy into available power. Recently, TENG,

Dr. B. Chen, Prof. Y. Yang, Prof. Z. L. Wang
Beijing Institute of Nanoenergy and Nanosystems
Chinese Academy of Sciences
Beijing 100083, China
E-mail: yayang@binn.cas.cn; zhong.wang@mse.gatech.edu

Dr. B. Chen, Prof. Y. Yang, Prof. Z. L. Wang
CAS Center for Excellence in Nanoscience
National Center for Nanoscience and Technology (NCNST)
Beijing 100190, China

Prof. Z. L. Wang
School of Materials Science and Engineering
Georgia Institute of Technology
Atlanta, GA 30332-0245, USA

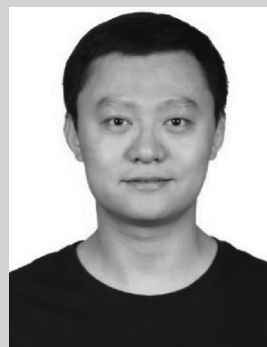
DOI: 10.1002/aenm.201702649

a novel technology, provides us a new method to go further in making use of the “uncontrollable” energy.^[38–40]

Triboelectrification is considered as generating electrostatic charges by the physical contact of two different materials’ surfaces.^[41–43] When the two materials are separated by mechanical force, a potential drop can compel the electrons to flow from the positive electrode onto negative electrode. Four fundamental working modes of the TENG, including vertical contact-separation mode, lateral sliding mode, single-electrode mode, and freestanding triboelectric-layer mode, have been reviewed in a previous article.^[44] As to the WD-TENG cases, the fundamental modes also can be included in these four modes, whereas all the WD-TENGs were designed to scavenge wind energy. Flutter-driven structure and rotational structure are the two typical structures that are selected to explain the working mechanism of WD-TENG in this article (**Figure 2**).

The theoretical model for the flutter-driven structure is illustrated in Figure 2a.^[31] This mode could also be classified into vertical contact-separation mode. Basically, Al and polytetrafluoroethylene (PTFE) are stacked face to face and regarded as two triboelectric materials. Al layer, deposited on Kapton, is not only considered as triboelectric material but also as electrode. The Al/Kapton/Al section vibrates up and down when external wind is applied, thus inducing the contact/separation state between Al and PTFE. At the initial state, the Al/Kapton/Al section is secluded by air gaps, and no output signal can be observed for both TEG 1 and TEG 2. When the Al/Kapton/Al section moves up to be in contact with the surface of PTFE, the positive and negative charges are generated accompanying with the electrons transferred from Al electrode onto PTFE film. The negative charges in this process can be conserved on PTFE film while the Al/Kapton/Al section oscillates down to access the underlying PTFE/Al film, whereas the positive charges on Al electrode directionally flow through external circuit owing to the electrostatic induction of the charged PTFE film, resulting in an output voltage and current signal from TEG 1.^[45] Both TEG 1 and TEG 2 will launch to proceed regular working mode from state (4) and go further in cycling the loop from state (4) to state (7). In this loop, both the top and bottom PTFE films maintain negative charges, meanwhile there are different amount of positive charges induced on Al electrodes when the Kapton film moves up and down, hence introducing an alternating voltage and current in external circuit for both TEG 1 and TEG 2. Apart from vertical contact-separation mode, flutter-driven WD-TENG can also be designed as a single-electrode mode by connecting one of the electrodes to the ground.^[25] Once the positive and negative parts are separated, the electrodes will preserve charges resulting in an electric potential difference between electrodes and ground, driving the electrons to flow corresponding to the direction from low potential to high potential. In this single-electrode mode, one of the triboelectric parts can vibrate freely without any restriction, therefore, widening the application of WD-TENG.

The electricity generating process of rotational structure is shown in Figure 2b. The structure of TENG mainly consists of two parts, a rotator and a stator. A layer of fluorinated ethylene propylene (FEP) serves as the rotator as well as negative triboelectric material, while the stator, regarded as positive triboelectric material, is composed of two isolated Cu electrodes. The



Bo Chen received his Bachelor’s degree in Chemical Engineering and Technology, and Ph.D. degree in Applied Chemistry both from Tianjin University, China. He was an exchange graduate student at the University of Wisconsin-Madison during 2014 to 2016. He is currently a postdoc fellow in Beijing Institute of Nanoenergy and Nanosystems, Chinese Academy of Sciences. His research currently focuses on developing nanogenerators for scavenging mechanical energy as well as water treatment and recycle.



Ya Yang received his Ph.D. in Materials Science and Engineering from University of Science and Technology Beijing, China. He is currently a professor at Beijing Institute of Nanoenergy and Nanosystems, CAS. His main research interests focus on the field of pyroelectric, piezoelectric, triboelectric, and thermoelectric nanogenerators for energy conversion, storage, and some novel applications.



Zhong Lin Wang is the Hightower Chair in Materials Science and Engineering and Regents’ Professor at Georgia Tech. He is also the chief scientist and director of the Beijing Institute of Nanoenergy and Nanosystems, Chinese Academy of Sciences. His discovery and breakthroughs in developing nanogenerators establish the principle and technological road map for harvesting mechanical energy from environment and biological systems for powering personal electronics. His research on self-powered nanosystems has inspired the worldwide effort in academia and industry for studying energy for micro-nanosystems, which is now a distinct disciplinary in energy research and future sensor networks.

process is classified as freestanding triboelectric-layer mode, which produces energy on account of contact electrification and electrostatic induction.^[46,47] An external mechanical force (e.g., finger taping) is essential to compel the rotator to be contacted with the stator. Since FEP possesses a higher electron affinity than Cu, electrons are injected from Cu electrodes onto

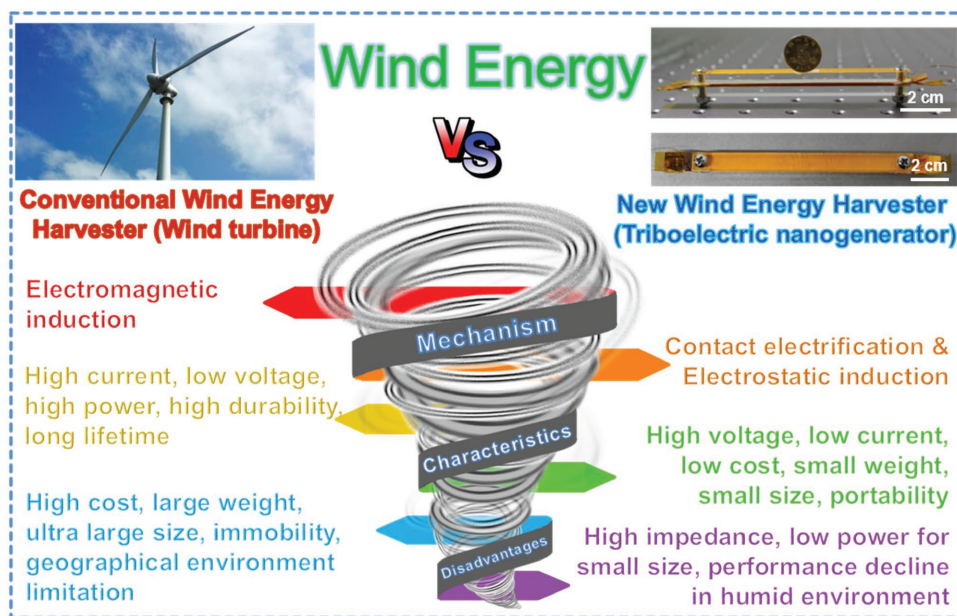


Figure 1. Comparison between conventional wind harvester (wind turbine) and new wind harvester (triboelectric nanogenerator). The inset picture on the left side is a typical wind turbine. Reproduced with permission.^[15] Copyright 2016, American Chemical Society. The inset picture on the right is a typical wind-driven triboelectric nanogenerator. Reproduced with permission.^[63] Copyright 2015, American Chemical Society.

FEP layers.^[48,49] Removing the external pressure, the rotator and the stator will fall into two parts and carry equal opposite triboelectric charge. Next, the rotator is aligned with the electrode 1 and 2 corresponding to the initial state and final state, respectively. When FEP layer approaches to or departs from whether electrode 1 or 2, an asymmetric charge distribution will be generated via electrostatic induction, causing the oscillated electrons motion between electrodes 1 and 2 to balance the local potential distribution. Thus, an AC current output can be obtained in response to the spinning circulation of the rotator movement. An in-plane sliding mode based WD-TENG can also be fabricated via a contact-friction structure compared to the contact-separate structure of freestanding triboelectric-layer mode.^[50]

Triboelectrification is a common phenomenon in our life, and almost all the materials, for instance, metal, glass, ceramic, and natural/artificial polymer, can show triboelectrification effect.^[51,52] Thus, all these materials are potential to fabricate TENG. Owing to different polarities, different materials possess different electron affinity, and the triboelectric ability of a series materials has been summarized.^[53] Considering the requirement of toughness, durability, and economic efficiency for WD-TENG, metal and artificial polymer are rendered as competitive candidates to achieve great output performance.^[54] **Figure 3a** shows some of the positive and negative materials used to manufacture WD-TENG and some of the reported triboelectric materials of WD-TENG are summarized in **Table 1**.

Efforts to enhance the output performance of WD-TENG are not only about the selection of triboelectric materials, but also the morphologies of material surfaces.^[55] Generally, coarse surface provides more contact area and possibility for triboelectrification to increase the friction force, resulting in more triboelectric charges. Physical and chemical techniques are adopted

to modify material surface to enhance the roughness and friction force. Some of the typical microstructures, like interwoven structure,^[56] nanowire structure,^[30] pyramid based structure,^[57] and more, are shown in **Figure 3**. Inductively coupled plasma etching is a common physical method to fabricate polymer nanowire to enhance the contact electrification.^[58] Meanwhile, diluted acid aqueous solution can be used as chemical etching agent to modify the surface of metal electrode.^[59] Therefore, from the triboelectric materials and the surface structure aspects, there are still plentiful methods to enhance the performance of WD-TENG, thus broadening practical applications.

3. Various Structures of WD-TENGs

Aiming to scavenge wind energy, flutter-driven structure and rotational structure are the two representative strategies applied to fabricate WD-TENG. Wind turbines and wind cups are utilized to convert wind energy into rotational mechanical motion in the system of rotational structure based WD-TENG. Meanwhile, based on the contact-separation between the flutter and the electrodes, flutter-driven WD-TENG simplifies the electrodes' structure as well as reduces the cost. Furthermore, other novel strategies have been exploited to diversify the structure and optimize the output performance of WD-TENG.

Flutter-driven structure WD-TENG was first reported by Yang et al., and that is recognized as a milestone via scavenging wind energy by a smart strategy.^[25] **Figure 4a,b** illustrates the structure of the TENG, that is, two layers of Al foils with a FEP film laying in midair. The FEP film is fixed only one side, leaving the other side as a free part. The Al foils serve as both triboelectric surfaces and electrodes, and are connected to ground respectively. When external wind is applied to the system, the

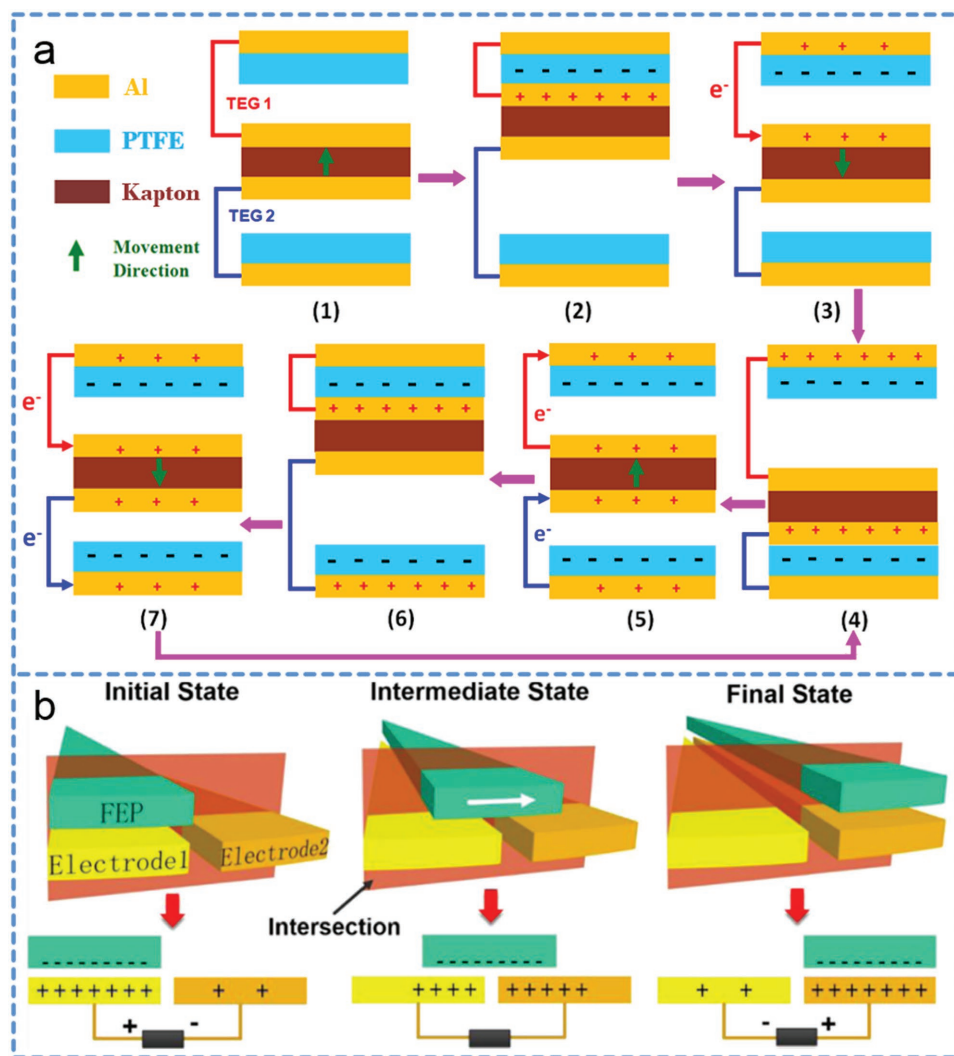


Figure 2. The typical working mechanisms of WD-TENG. a) The flutter-driven structure (Reproduced with permission.^[31] Copyright 2015, Wiley-VCH) and b) the rotational structure (Reproduced with permission.^[30] Copyright 2015, Elsevier).

freestanding side of the FEP film will vibrate up and down to contact the surfaces of both Al electrodes, leading to an output voltage and current across an external resistor. Output voltage and current are up to 100 V and 1.6 μ A, and a corresponding output power of 0.16 mW are detected under a loading resistance of 100 M Ω .

Although single-side fixed based WD-TENG holds a great number of advantages in harvesting wind energy, it still undergoes instability of the output electric signal due to the arbitrary fluttering of the freestanding electrode. Aero-elastic motion mode WD-TENG, whose flutter is fixed on both two sides, was designed to provide new approach to overcome this shortage. Figure 4c presents the schematic diagram of the double-side-fixed mode WD-TENG. Basically, the WD-TENG consists of two Al electrodes covered by superhydrophobic films and a polyamide (PA) film. Two air gaps divide two modified Al electrodes and PA film which is fixed by two bolts into three parts. The air fluid is loaded into the gaps and vibrates the PA film, resulting in the contact and separation of the superhydrophobic

films and PA film, thus generating an output voltage and current. A photograph of the fabricated WD-TENG is as shown in Figure 4d.

The rotational structure is widely used to scavenge wind energy via using wind turbines or wind cups. As shown in Figure 2b, typical in-plane cycled sliding mode WD-TENG consists of a rotator (FEP) and a stator with two separated electrodes (Cu). FEP and Cu, with opposite triboelectric polarities, are initially compelled to contact each other. When the two planes are relatively sliding, electrons transfer from the surface of Cu onto FEP plane, leading to an output electric signal. In order to enhance the output performance, the non-contact working mode are more preferred rather than contact-separation working mode, since the latter mode is always suffered from the friction effect which reduces the energy convert efficiency.^[60]

A rotational sweeping based WD-TENG was developed for harvesting weak wind energy in the environment.^[61] The main structure of the WD-TENG includes a framework, a shaft, a

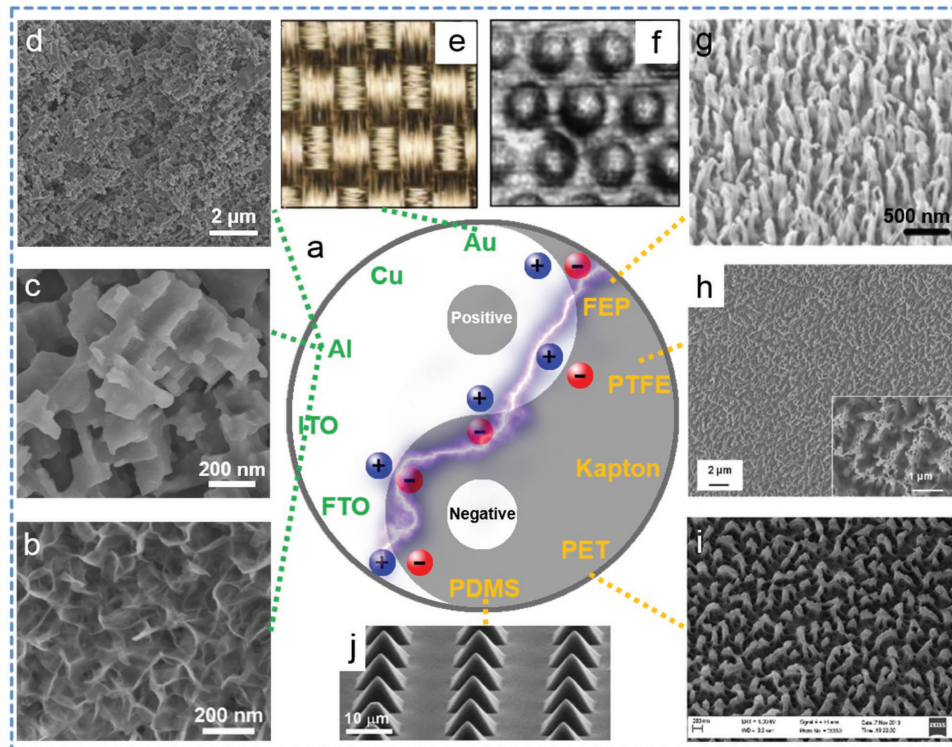


Figure 3. Various triboelectric materials and their microstructures. a) The positive and negative materials used to manufacture WD-TENG. b) A SEM image of Al film surface modified by immersing it in hot deionized water at 120 °C for 20 min. Reproduced with permission.^[80] Copyright 2014, Springer. c,d) SEM images of etched Al electrode and treated with fluoride with different magnifications. Reproduced with permission.^[59] Copyright 2016, American Chemical Society. The structure of e) a flexible Au-coated woven flag and f) a rigid PTFE counter plate. Reproduced with permission.^[56] Copyright 2014, Nature Publishing Group. g) A SEM image of the FEP polymer nanowires. Reproduced with permission.^[30] Copyright 2015, Elsevier. h) A SEM image of the PTFE film with nanowire-like structures etched by inductively coupled plasma (ICP) process. Reproduced with permission.^[61] Copyright 2013, American Chemical Society. i) Surface of PET film etched with ICP process. Reproduced with permission.^[58] Copyright 2016, Wiley-VCH. j) A SEM image of the micro-pyramid-exposed polydimethylsiloxane (PDMS) array. Reproduced with permission.^[57] Copyright 2015, Elsevier.

flexible rotor blade, and two stators. When wind is applied to the conventional wind cup, a flexible and soft polyester (PET) rotor blade with a PTFE film adhered at the end will periodically sweep across the Al electrodes. In this process, the PTFE film consecutively contacts and separates from Al electrodes, serving as the basic process for generating electricity.

Besides the flutter-driven structure and rotational structure, other novel WD-TENG structures have been exploited to satisfy the requirement in various complicated condition. In particular, a miniaturized structure WD-TENG is necessitated in order to integrate the wind harvest with mobile devices. A thin film membrane based WD-TENG is a promising new generation of wind energy harvester making both miniaturized device area and high performance come true. A vertically stacked thin-film WD-TENG was invented and the structure is illustrated in Figure 4e.^[57] The WD-TENG includes two rigid Al electrodes and a vibrating membrane which consists of an intercalated Al film sandwiched by two micro-pyramid-exposed polydimethylsiloxane (PDMS) on both the top and bottom sides. Air gaps between the Al electrodes and inner PDMS membrane are formed by placing spacers made of overlapped Kapton films. A narrow air gap is crucial to reduce device size, enhance effective contact area, and increase mechanical robustness. Figure 4f shows three membranes can be arrayed in a row to enhance

output power. If each of the WD-TENG is in the form of a cross stack, i.e., perpendicular to each other, bi-directional wind energy can be fully utilized.

A lawn structure based, flexible and transparent WD-TENG, as displayed in Figure 4g, is presented to harvest energy from natural wind at arbitrary wind blowing direction.^[58] A unit of vertically freestanding polymer strips is fabricated by a PET thin film coated with indium tin oxide (ITO) on one side. The laminar WD-TENGs are arrayed as a kelp forest morphology and each single strip can sway independently to achieve a contact-separation process to each other when natural wind passes by. Thus, each contact between two adjacent strips can deliver an output signal. Plenty of strips orderly stand to form an environmental wind energy harvesting system. This system offers a novel approach for scavenging wind energy as well as a solid step toward self-powered home technology.

The flag structure which can be folded, bent, and even twisted in the air is considered as a novel strategy to harvest wind energy to take place the conventional wind turbine due to its high cost of manufacturing and installation. In addition, in some extreme environment, such as high-altitude places, traditional wind power technology is no longer suitable for working. An innovative flag structure based freestanding woven WD-TENG is exploited to harvest high-altitude wind energy from

Table 1. A summary of triboelectric materials and output performance of various WD-TENGs.

Structures	Triboelectric materials	Voltage [V]	Current [μ A]	Power [mW]	Ref.
Rotational sweeping mode	Al and PTFE	250	250	62.5	[61]
Single-side-fixed mode	Al and FEP	100	1.6	0.16	[25]
Rotational sweeping mode	Al and PTFE	55	–	0.03	[28]
Single-side-fixed mode	Au and PTFE	200	60	0.86	[56]
Single-side-fixed mode	FTO and PTFE	36	4.1	–	[29]
Single-side-fixed mode	Cu and PTFE	225	23	1.5	[33]
In-plane cycled sliding mode	Cu and Kapton	320	3400	–	[32]
Double-side-fixed mode	Cu and PTFE	342	140	–	[63]
Single-side-fixed mode	Al and PTFE	400	60	3.7	[31]
Single-side-fixed mode	Cu and PTFE	–	55.7	3.5	[34]
In-plane cycled sliding mode	Cu and FEP	\approx 15	\approx 6	–	[30]
Double-side-fixed mode	Al and PTFE	334	67	5.5	[81]
Double-side-fixed mode	Cu and FEP	375	260	26	[15]
Lawn structure	ITO and PET	78	16.3	–	[58]
Double-side-fixed mode	PA and FDCS	218	30	2.2	[59]
Flag structure	Ni and Kapton	40	30	–	[62]
Double-side-fixed mode	Cu and FEP	51	40	1.7	[35]

arbitrary directions (Figure 4h).^[62] Ni-coated polyester textiles (Ni belts) and Kapton film sandwiched Cu belts (KSC belts) are knitted together to form a woven structure. To be specific, the polyester is coated by Ni on both top and bottom sides, and all the Ni belts are connected as one electrode. Meanwhile, the Cu foil is covered by Kapton film on both sides, and all the KSC belts are connected as the other electrode. It is clear that an air gap is left in each woven unit between two electrodes to realize the contact-separation process driven by wind, leading to an output signal by a coupled effect of contact electrification and electrostatic induction. This flag structure based WD-TENG has great potential for applications at high altitude, for instance, weather/environmental sensing systems.

4. Output Performances and Enhancement of WD-TENG

Output performance is one of the most important indicators, since it dramatically affects the application of WD-TENG. The materials and corresponding output performances of various WD-TENG are summarized in Table 1. The ranges of output voltage and current are 1.5–400 V (with a size of $22 \times 10 \times 67 \text{ mm}^3$) and 1.6 μ A to 3.4 mA (with a radius of 70 mm), respectively. It is well known that the contact area, as well as friction materials, can significantly influence triboelectric performance of TENG. Besides, the working modes also play an important role in harvesting wind energy. For instance, contact and noncontact working states were investigated to show the difference for the output performance and lifetime of the WD-TENGs.^[60] The highest output performance can be observed from the contact state due to the constant surface charge generation and the most effective electrostatic induction, while the surface wear can be effectively minimized, thus

dramatically enhance the stability and lifetime for WD-TENG in noncontact free-rotating state.

Device size, one of the most important parameters, determines the output performances of WD-TENG to some degree. The relationship between the output properties and different sizes of the devices were investigated to achieve the largest output performance.^[31] As shown in Figure 5a, the output voltage and current reach the maximum value at the height of 10 mm. Increasing the length of Kapton film, both output voltage and current improve consistently, where the length of the device is about 57 mm (Figure 5b). As depicted in Figure 5c, the output voltage approaches the largest value which is about 400 V, where the corresponding output current is about 60 μ A. In addition, the working frequency linearly increases as the air-flow rate increases from about 7.5 to about 22 m s^{-1} (Figure 5d). Besides, the device width and the vibrating film thickness were also investigated to realize the largest output performance.^[63]

Although WD-TENG can attain a voltage as high as 400 V, it is still a challenge to obtain an output current high enough to satisfy the requirement of electric equipment. One of the promising strategies to overcome the low output power is to integrate several WD-TENGs to enhance the output performance. The output voltage and short-circuit current of a single WD-TENG are displayed in Figure 5e,f.^[63] After integrating ten rectified WD-TENG with the connections in parallel as presented in Figure 5g, the total output current can achieve as high as 550 μ A compared to 160 μ A which is the output current of a single WD-TENG (Figure 5h). However, because of the vertical oscillation of each point on the fluttering film, different parts of the film exert partially counteracting effects on the variation of electric potential, making WD-TENG suffer from a large diminishment of electric output. As a consequence, another smart strategy of segmenting the electrode into a linear array of strip-shaped units with uniform width was developed, which can

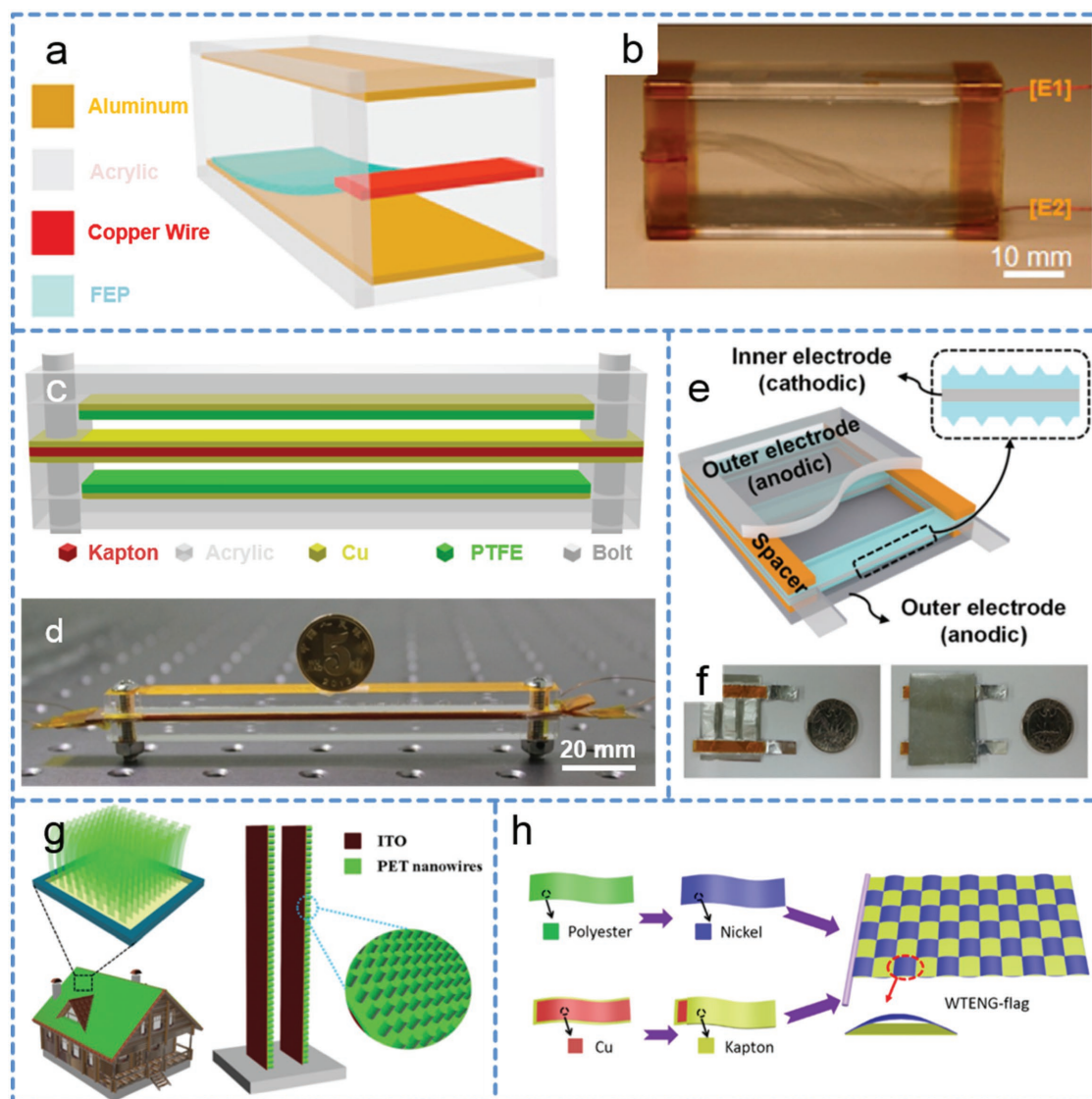


Figure 4. Various structures of WD-TENG. a,b) The structure and photograph of the first reported flutter-driven mode WD-TENG. Reproduced with permission.^[25] Copyright 2013, American Chemical Society. c,d) The schematic diagram and a photograph of the WD-TENG. Reproduced with permission.^[63] Copyright 2016, American Chemical Society. e,f) Schematic of a single-layer vertically stacked structure WD-TENG and its photograph. Reproduced with permission.^[57] Copyright 2015, Elsevier. g) Schematic of the lawn structure WD-TENG and it can easily be equipped to the rooftops for scavenging natural wind energy. Reproduced with permission.^[58] Copyright 2016, Wiley-VCH.

significantly increase the output current over 500% compared to the structure without the segmentation.^[64]

5. WD-TENG Hybridized with Other Types of Generators

Other than size enlargement, device integration and segmented structure electrode modification, the strategy of hybridizing with other forms of generators, is explored aiming to sustainably power some electronic devices with large power demand. In general, other types of energy sources including electromagnetic generator (EMG), solar cell, piezoelectric nanogenerator (PiENG), and pyroelectric nanogenerator (PyENG) can

be combined with TENG to achieve a win-win situation, which means a higher output performance will be obtained compared to every single energy source.

As discussed above, the typical flutter-driven structure WD-TENG possesses two immobile electrodes with an air gap allowing a fluttering film lying in the middle of the electrodes. Upon this structure, the up and down film gives the system a chance to utilize electromagnetic induction to produce induction current, which can be designed as an EMG. As presented in **Figure 6a**, a hybridized nanogenerator, including two TENGs at the freestanding end and two EMGs at the front section of the device, was fabricated to convert the kinetic energy of the air flow into electric energy for sustainably powering temperature sensor.^[34] The hybridized nanogenerator can generate

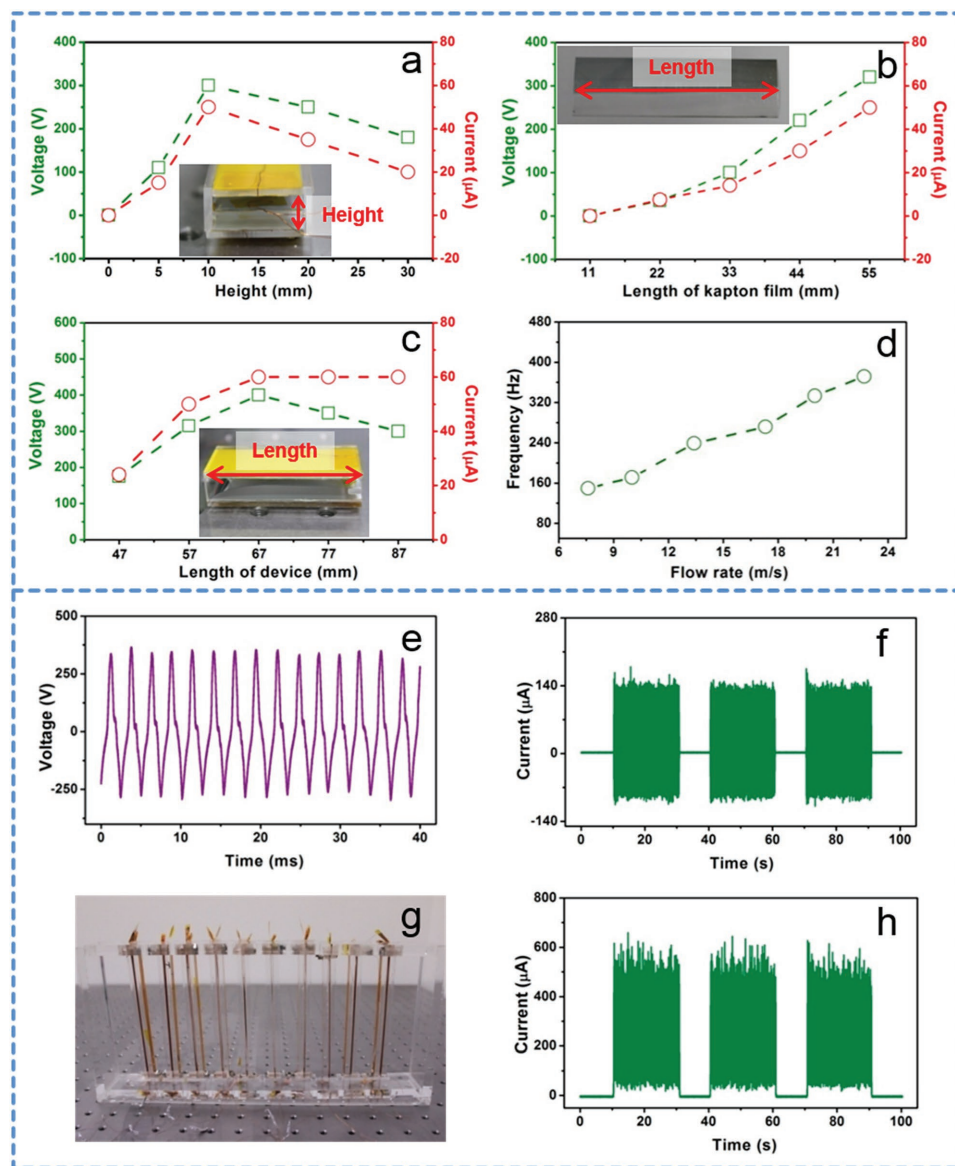


Figure 5. The output performance and enhancement of WD-TENGs. a–c) Dependence of rectified open-circuit voltage and short-circuit current of the device on the device height, the length of the Kapton film, and the device length. d) The working frequencies of WD-TENG under different flow rates. Reproduced with permission.^[31] Copyright 2015, Wiley-VCH. e) The output voltage and f) short-circuit current of the WD-TENG. g) The photograph and h) short-circuit current of ten WD-TENGs connected in parallel. Reproduced with permission.^[63] Copyright 2015, American Chemical Society.

output power up to 3.5 and 1.8 mW under an air-flow speed of about 18 m s^{-1} for each single TENG and EMG, respectively. The rectified output current signals of TENG with transformer, EMG, and TENG/EMG with transformer are shown in Figure 6b, indicating inconspicuous current enhancement can be noted for the hybridized nanogenerator as compared with the individual TENG or EMG, which can be ascribed to the asynchronism for the TENG and EMG.

Nanogenerator can also provide new methods to realize the sustainable energy supply in a smart city by hybridizing WD-TENG with solar cells. As illustrated in Figure 6c, a WD-TENG and solar cell composite nanogenerator was explored to scavenge energy from the city environment for powering some electric devices.^[15] The WD-TENG and solar cell can be

installed on the roofs of buildings to individually or simultaneously scavenge wind and solar energy (Figure 6d). According to the same device area of about $120 \times 22 \text{ mm}^2$, the output power of the WD-TENG and solar cell can be up to 26 and 8 mW, respectively. Figure 6e demonstrates that the hybrid nanogenerator generates the largest output current (about 12 mA) as compared to individual WD-TENG (about 9 mA) and solar cell (about 4 mA).

Except combining WD-TENG with EMG or solar cell, it is highly desirable to hybridize WD-TENG with other kinds of mechanical energy as well as thermal energy to scavenge these two forms of energy from the environment at the same time. As displayed in Figure 6f, a hybrid nanogenerator consists of a polyvinylidene fluoride (PVDF) nanowires–PDMS composite

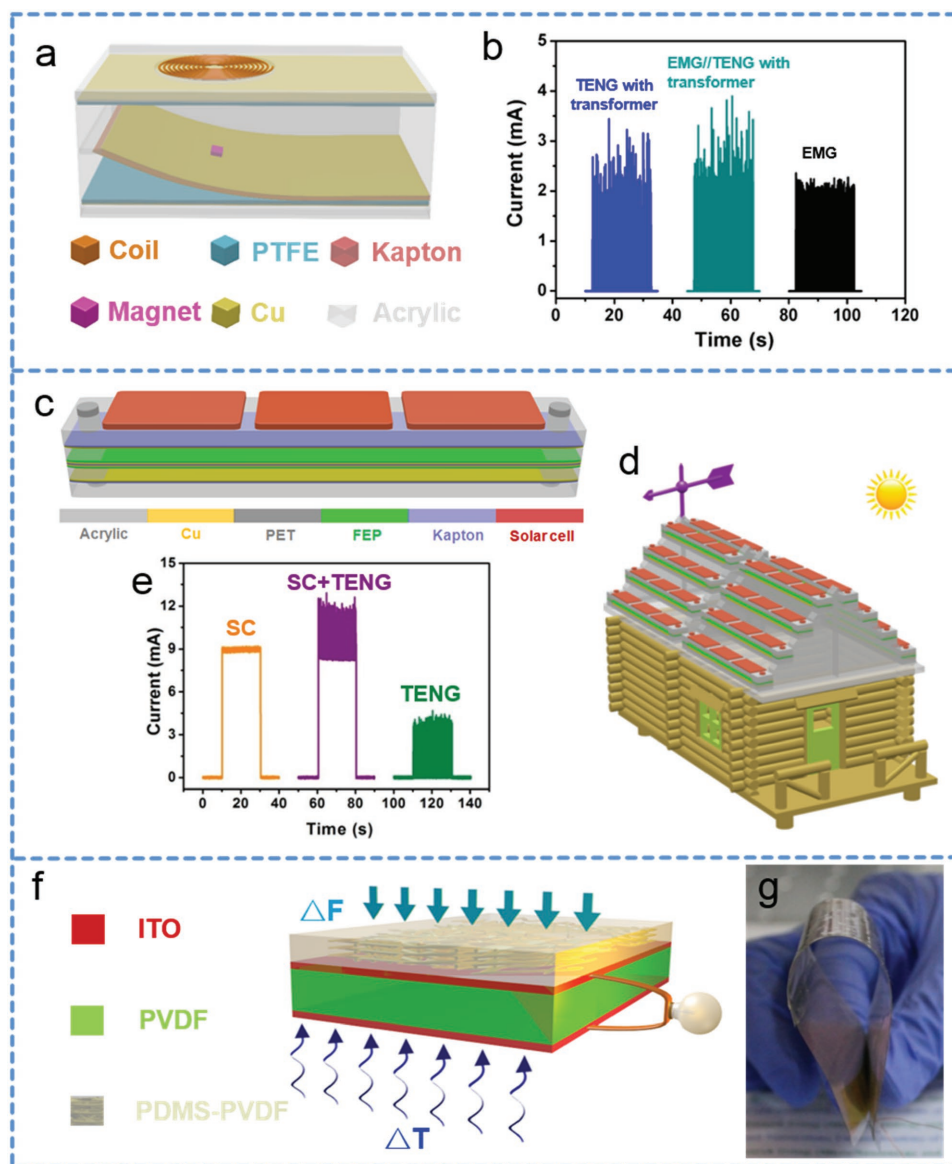


Figure 6. WD-TENG hybridized with other generators. a) The schematic diagram of the hybridized EMG/TENG device. b) The rectified output current signal of EMG, TENG, and EMG/TENG. Reproduced with permission.^[34] Copyright 2015, American Chemical Society. c) The schematic diagram of the hybridized solar cell/TENG device. d) The schematic diagram of the integrated hybridized solar cell/TENG on the roof of a house model. e) The output current signals of solar cell, TENG, and solar cell/TENG. Reproduced with permission.^[15] Copyright 2016, American Chemical Society. f) The schematic diagram of the hybridized PiENG/PyENG/TENG. g) A photograph of the flexible hybridized nanogenerator. Reproduced with permission.^[65] Copyright 2016, Wiley-VCH.

film and a poled PVDF film with the ITO electrodes on both surfaces, which can scavenge mechanical and thermal energy by using triboelectric, piezoelectric, and pyroelectric effects.^[65] The TENG-PiENG and the PyENG are integrated together into one device and same output electrode. A flexible nylon film was utilized as an oscillating membrane to produce the periodic contact and separation between nylon film and PVDF nanowires-PDMS composite film to achieve triboelectric output signal. When an external force load was applied to compress or stretch on the poled PVDF film, the piezoelectric unit can offer a piezoelectric output signal. Moreover, the temperature fluctuation of the poled PVDF film will affect the spontaneous

polarization, and the spontaneous polarization can compel electrons to flow between the two ITO electrodes, thus leading to a pyroelectric output signal. Figure 6g shows the flexibility of the hybrid nanogenerator.

6. Applications of WD-TENG

WD-TENG is a basically physical process converting wind/air-flow energy into electricity through the triboelectrification and electrostatic induction processes. The high output voltage endows WD-TENG amount of practical application. One of

the major applications, apparently, is powering electric devices by use of the output electric signals from WD-TENG. The resulting electric energy can also be stored in energy storage equipment, for instance, capacitor and Li-ion battery, as a secondary energy source. Moreover, as a self-sufficient, high-efficient power source, WD-TENG has been involved in various self-powered systems by collecting wind energy from ambient environment. The applications of WD-TENG in different fields have been briefly summarized in this section.

The WD-TENG can be utilized as a power source for running some electric devices.^[66] However, sometime the integration of WD-TENG is crucial to meet the large power demand in some situation. Several typical applications have been summarized in **Figure 7a**. Ten light-emitting diodes (LEDs) connected in series were simultaneously lighted up through directly connecting to the integrated ten WD-TENGs driven by the external air flow, as shown in the figure. The printed text can be visible in a completely dark environment in use of the illumination of LEDs.^[31] An integrated nanogenerators system can be installed on the roofs of city house to provide urban illumination.^[15] A white globe light bulb can be directly driven by WD-TENGs and hence providing sufficient light intensity of about 43 lx for reading text.^[63] Furthermore, a temperature sensor system for sustainably measuring human body temperature was accomplished through scavenging human nose blowing induced low air-flow energy by WD-TENG. In addition, a smart wireless sensor node system which is composed of a WD-TENG, a power management circuit, a 10 mF capacitor, a wireless smart temperature sensor node, and an iPhone was fabricated to monitor environment temperature and then send data to iPhone for further analysis. The wireless smart temperature sensor can measure the temperature of a human finger and show a value of 30.37 °C on an iPhone through a wireless connection.

The output current derived from WD-TENG is alternating current power, which in some degree limits WD-TENG's application in some situation. Much effort has been devoted toward converting alternating current into direct current, and hence the capacitor and battery technology are introduced to overcome this problem. Under an air-flow velocity of 15 m s⁻¹, a dual-plate flag structure WD-TENG with a size of 7.5 × 5 cm² can fully charge a 100 μF capacitor within 4 min.^[56] Meanwhile, a TiO₂ nanotube array based Li-ion battery can be charged from 0.2 to 2.1 V within 10 min by using a hybrid nanogenerator, leading to a total electrical capacity of about 11.7 μAh.^[15]

Assembled with other electric devices as various self-power systems, WD-TENG is expected to be utilized in different conditions, which represents an important step forward to practical applications.^[67] A WD-TENG based self-power humidity sensor has been designed, and the variation of output voltage or current can denote the relative humidity of different environment (20%–100%) at a fixed air-flow rate.^[29] Another common WD-TENG based self-power system is the wind speed sensor. Zhang et al. fabricated a wind energy harvesting and sensor system to demonstrate the application of the WD-TENG as a self-power wind speed sensor.^[28] The output voltage can approach as high as about 23 V at a wind speed of 32.6 m s⁻¹. Gas sensing is widely used in life science, security, and environmental protection. Detecting alcohol is one of the important aspects in gas sensing territory, which is vital for safety and drunk driving

testing. An active alcohol breath analyzer has been developed based on the blow-driven TENG technology.^[30] Regardless the air-flow speed, there is a proportional relationship between the blow air induced voltage across the sensor and the breathed-out alcohol concentration. Due to a low sensor resistance, the induced voltage drop across the sensor is almost zero when the alcohol analyzer was being blown by a tester without drinking alcohol. In contrary, the alcohol vapor will dramatically increase the resistance of the sensor, leading to an obvious voltage variation which can trigger a siren. In addition, the alcohol analyzer also possesses outstanding selectivity for alcohol, fast response time (11 s), as well as a fast recovery period (20 s). Another important application of WD-TENG should be noted, which is detection of motion as a sensor. Three typical different stages of a car motion (i.e., acceleration, uniform motion, and deceleration) can be observed through a WD-TENG setup.^[60]

7. Outlook

Since wind energy is free, clean, renewable, and sustainable, it has been considered as one of the most promising energy forms to fight with global energy crisis. WD-TENG is a newly developed exciting technology which can convert the wind power into usable energy forms, namely, electricity. In this review, we have systematically summarized the triboelectric materials and various structures as well as the output performance of different WD-TENGs. WD-TENG, as a single device, can generate an outstanding output voltage as high as 400 V (with a size of 22 × 10 × 67 mm³). In addition, WD-TENGs can be hybridized with other forms of power generators, such as solar cells, EMGs, and PiENGs, which can widen their applied environment and field. Besides, WD-TENG has shown many advantages including low-cost, high efficiency, sustainability, availability, and easy fabrication, making it potential to be utilized as self-power electronics.

The development of WD-TENG in future will follow the trend of integration, miniaturization, and diversification. Individual WD-TENG will be encouraged to be integrated as a large-scale wind power plant for generating enough electricity to cater the large power demand in some cases, especially in some open area where wind power is strong and steady. **Figure 7b** is an illustrative diagram that shows how we can construct a WD-TENG based power plant. A great many of WD-TENGs can first be integrated as a wall, and then a large area of “electric walls” can be arranged as an array for scavenging wind energy. After being transformed by power substations, the collective electric power can be transported through cables for further electricity supplement. A 100 × 100 m² “electric wall” (including around 10⁷ individual WD-TENGs with a unit power of 26 mW) can supply a total electric power output around 260 kW. Even though WD-TENG possessed relative lower output power compared with wind turbine, we can also see its own inspiring advantages including high voltage, low cost, as well as small weight. On the contrary, it is also essential to minimize the size of WD-TENG in some situations to fabricate wearable electronics, flexible electronics, and sensor networks.^[68–70] Moreover, not only the small size, but also the sensitivity of WD-TENG is necessary to be carefully considered, which means micro- or nanostructures

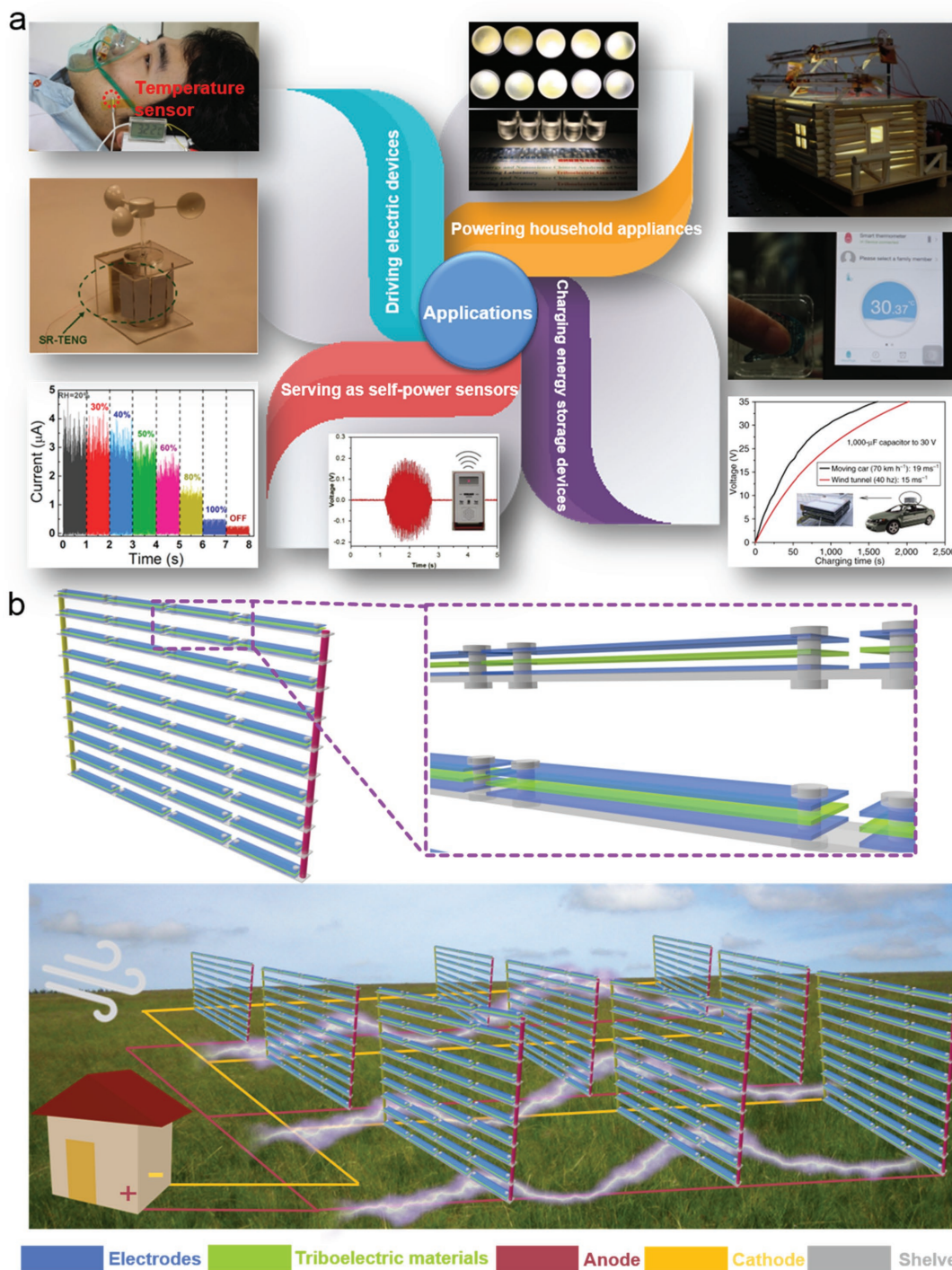


Figure 7. Illustration of various applications for WD-TENG. a) A summary of various applications for WD-TENGs, including powering LEDs (Reproduced with permission.^[31] Copyright 2015, Wiley-VCH), spot light (Reproduced with permission.^[63] Copyright 2015, American Chemical Society), temperature sensor (Reproduced with permission.^[59] Copyright 2016, American Chemical Society), humidity sensor (Reproduced with permission.^[29] Copyright 2014, American Chemical Society), wind speed sensor (Reproduced with permission.^[28] Copyright 2013, American Chemical Society), and alcohol sensor (Reproduced with permission.^[30] Copyright 2015, Elsevier). b) An illustrative diagram for large-scale “electric walls” farm land.

may give novel WD-TENG a chance to detect slight air-flow fluctuations. These micro- or nanostructures based WD-TENG can be used in precise instruments for human health care, meteorological monitoring, and military equipment.^[44,71–75]

Besides, based on the fundamental mechanism of TENG, different triboelectric materials and structures of WD-TENG are urgently required to be explored to be used in some special environments. For example, in high vacuum environment, the

charge density of TENG can be boosted without the limitation of air breakdown.^[76] WD-TENG is expected to work not only in atmosphere but also in aerospace, which requires WD-TENG can scavenge “wind energy” produced by other forms of fluid, such as solar wind, rather than air flow. At the same time, WD-TENG is also required to undergo harsh environment, such as ultralow temperature, rough vacuum, intense radiation, and zero gravity.^[77–79] Another key issue, the lifetime of WD-TENG, should be noted to eliminate people’s concern about the cost of maintenance and material consumption. The output voltage and current stability of the WD-TENG has been investigated in previous research by keeping the device continuously working under a wind load for 14 h.^[59] No obvious decrease of the output signals can be observed indicating a couple of hours effective lifetime. As to the stability on the scale of few months even years, there is no relative research reporting such a long period of experiment as far as we know. Therefore, much efforts are encouraged to donate in future in order to illustrate the practicability of the WD-TENG.

Despite significant improvements have been achieved since the first WD-TENG was reported in 2013,^[61] there are tremendous room for growth in terms of scavenging wind energy by TENG. As a prerequisite to further develop, several main issues are essential to be addressed: (1) thoroughly comprehending the fundamental mechanism of triboelectrification is necessary and it is also the basis of the development of WD-TENG. Better understanding the charge transfer process will guide people to further optimize output performance and applications of WD-TENG. (2) The triboelectric materials are needed to be largely optimized and improved. The abrasion of materials is inevitable during the triboelectrification, and how to improve durability and extend working life of devices are crucial to widen the application of WD-TENG, especially in some harsh environments. Moreover, lighter and flexible devices may be preferred in some situations to meet the demand of portability. (3) Enhancing the energy conversion efficiency is still a challenge for improving the output performance of WD-TENG. (4) The cost of WD-TENG fabrication is still relative high for large-scale integration. In future, more efforts are necessary to be placed on reducing the cost of materials for widespread commercial applications. Showing an overview of this technology, we hope WD-TENG will attract more attention to this field, and encourage more profound investigation. With the advantages of new materials and integrated technologies development, the commercialization of high-performance and low-cost WD-TENG will be applied as a new generation power source and widespread all around the world.

Acknowledgements

B.C. and Y.Y. contributed equally to this work. The authors acknowledge the support from the National Key R&D Program of China (Grant Nos. 2016YFA0202701 and 2016YFA0202704), the National Natural Science Foundation of China (Grant Nos. 51472055, 61404034, 51432005, 5151101243, and 51561145021), External Cooperation Program of BIC, Chinese Academy of Sciences (Grant No. 121411KYS820150028), the 2015 Annual Beijing Talents Fund (Grant No. 2015000021223ZK32), Beijing Municipal Science & Technology Commission (Grant No. Y3993113DF), and the “thousands talents” program for the pioneer researcher and his innovation team, China.

Conflict of Interest

The authors declare no conflict of interest.

Keywords

hybrid energy cells, Li ion batteries, triboelectric materials, triboelectric nanogenerator, wind energy

Received: September 21, 2017

Revised: October 19, 2017

Published online:

- [1] T. A. Carleton, S. M. Hsiang, *Science* **2016**, 353, aad9837.
- [2] Y. Qin, X. Wang, Z. L. Wang, *Nature* **2008**, 451, 809.
- [3] M. I. Hoffert, K. Caldeira, G. Benford, D. R. Criswell, C. Green, H. Herzog, A. K. Jain, H. S. Khesghi, K. S. Lackner, J. S. Lewis, *Science* **2002**, 298, 981.
- [4] J. Chen, Y. Huang, N. Zhang, H. Zou, R. Liu, C. Tao, X. Fan, Z. L. Wang, *Nat. Energy* **2016**, 1, 16138.
- [5] X. Wang, J. Song, J. Liu, Z. L. Wang, *Science* **2007**, 316, 102.
- [6] S. Wang, Y. Xie, S. Niu, L. Lin, Z. L. Wang, *Adv. Mater.* **2014**, 26, 2818.
- [7] C. Bowen, H. Kim, P. Weaver, S. Dunn, *Energy Environ. Sci.* **2014**, 7, 25.
- [8] Z. L. Wang, T. Jiang, L. Xu, *Nano Energy* **2017**, 39, 9.
- [9] G. J. Herbert, S. Iniyar, E. Sreevalsan, S. Rajapandian, *Renewable Sustainable Energy Rev.* **2007**, 11, 1117.
- [10] S. Xu, Y. Qin, C. Xu, Y. Wei, R. Yang, Z. L. Wang, *Nat. Nanotechnol.* **2010**, 5, 366.
- [11] S. Chu, A. Majumdar, *Nature* **2012**, 488, 294.
- [12] R. Wiser, K. Jenni, J. Seel, E. Baker, M. Hand, E. Lantz, A. Smith, *Nat. Energy* **2016**, 1, 16135.
- [13] T. Ackermann, L. Söder, *Renewable Sustainable Energy Rev.* **2000**, 4, 315.
- [14] D. M. Kammen, D. A. Sunter, *Science* **2016**, 352, 922.
- [15] S. Wang, X. Wang, Z. L. Wang, Y. Yang, *ACS Nano* **2016**, 10, 5696.
- [16] F.-R. Fan, Z.-Q. Tian, Z. L. Wang, *Nano Energy* **2012**, 1, 328.
- [17] Y. Yang, Z. L. Wang, *Nano Energy* **2015**, 14, 245.
- [18] T. Quan, X. Wang, Z. L. Wang, Y. Yang, *ACS Nano* **2015**, 9, 12301.
- [19] Y. Yang, H. Zhang, Z. L. Wang, *Adv. Funct. Mater.* **2014**, 24, 3745.
- [20] G. Zhu, Z.-H. Lin, Q. Jing, P. Bai, C. Pan, Y. Yang, Y. Zhou, Z. L. Wang, *Nano Lett.* **2013**, 13, 847.
- [21] L. C. Rome, L. Flynn, E. M. Goldman, T. D. Yoo, *Science* **2005**, 309, 1725.
- [22] J. M. Donelan, Q. Li, V. Naing, J. Hoffer, D. Weber, A. D. Kuo, *Science* **2008**, 319, 807.
- [23] H. Zhang, Y. Yang, Y. Su, J. Chen, K. Adams, S. Lee, C. Hu, Z. L. Wang, *Adv. Funct. Mater.* **2014**, 24, 1401.
- [24] P. Bai, G. Zhu, Z.-H. Lin, Q. Jing, J. Chen, G. Zhang, J. Ma, Z. L. Wang, *ACS Nano* **2013**, 7, 3713.
- [25] Y. Yang, G. Zhu, H. Zhang, J. Chen, X. Zhong, Z.-H. Lin, Y. Su, P. Bai, X. Wen, Z. L. Wang, *ACS Nano* **2013**, 7, 9461.
- [26] G. Cheng, Z.-H. Lin, Z.-L. Du, Z. L. Wang, *ACS Nano* **2014**, 8, 1932.
- [27] Y. Hu, C. Xu, Y. Zhang, L. Lin, R. L. Snyder, Z. L. Wang, *Adv. Mater.* **2011**, 23, 4068.
- [28] H. Zhang, Y. Yang, X. Zhong, Y. Su, Y. Zhou, C. Hu, Z. L. Wang, *ACS Nano* **2013**, 8, 680.
- [29] H. Guo, J. Chen, L. Tian, Q. Leng, Y. Xi, C. Hu, *ACS Appl. Mater. Interfaces* **2014**, 6, 17184.
- [30] Z. Wen, J. Chen, M.-H. Yeh, H. Guo, Z. Li, X. Fan, T. Zhang, L. Zhu, Z. L. Wang, *Nano Energy* **2015**, 16, 38.

- [31] S. Wang, X. Mu, Y. Yang, C. Sun, A. Y. Gu, Z. L. Wang, *Adv. Mater.* **2015**, *27*, 240.
- [32] S. Chen, C. Gao, W. Tang, H. Zhu, Y. Han, Q. Jiang, T. Li, X. Cao, Z. Wang, *Nano Energy* **2015**, *14*, 217.
- [33] H. Guo, X. He, J. Zhong, Q. Zhong, Q. Leng, C. Hu, J. Chen, L. Tian, Y. Xi, J. Zhou, *J. Mater. Chem. A* **2014**, *2*, 2079.
- [34] X. Wang, S. Wang, Y. Yang, Z. L. Wang, *ACS Nano* **2015**, *9*, 4553.
- [35] X. Wang, Y. Yang, *Nano Energy* **2017**, *32*, 36.
- [36] T. Quan, Z. L. Wang, Y. Yang, *ACS Appl. Mater. Interfaces* **2016**, *8*, 19573.
- [37] X. Wang, Z. L. Wang, Y. Yang, *Nano Energy* **2016**, *26*, 164.
- [38] X. Zhong, Y. Yang, X. Wang, Z. L. Wang, *Nano Energy* **2015**, *13*, 771.
- [39] K. Zhang, X. Wang, Y. Yang, Z. L. Wang, *ACS Nano* **2015**, *9*, 3521.
- [40] K. Zhang, Y. Yang, *Nano Res.* **2016**, *9*, 974.
- [41] W. Tang, T. Jiang, F. R. Fan, A. F. Yu, C. Zhang, X. Cao, Z. L. Wang, *Adv. Funct. Mater.* **2015**, *25*, 3718.
- [42] S. Kim, M. K. Gupta, K. Y. Lee, A. Sohn, T. Y. Kim, K. S. Shin, D. Kim, S. K. Kim, K. H. Lee, H. J. Shin, *Adv. Mater.* **2014**, *26*, 3918.
- [43] Z. L. Wang, *Faraday Discuss.* **2015**, *176*, 447.
- [44] Z. L. Wang, J. Chen, L. Lin, *Energy Environ. Sci.* **2015**, *8*, 2250.
- [45] F. Saurenbach, D. Wollmann, B. Terris, A. Diaz, *Langmuir* **1992**, *8*, 1199.
- [46] J. Chen, G. Zhu, W. Yang, Q. Jing, P. Bai, Y. Yang, T. C. Hou, Z. L. Wang, *Adv. Mater.* **2013**, *25*, 6094.
- [47] G. Zhu, B. Peng, J. Chen, Q. Jing, Z. L. Wang, *Nano Energy* **2015**, *14*, 126.
- [48] G. Zhu, P. Bai, J. Chen, Z. L. Wang, *Nano Energy* **2013**, *2*, 688.
- [49] W. Yang, J. Chen, Q. Jing, J. Yang, X. Wen, Y. Su, G. Zhu, P. Bai, Z. L. Wang, *Adv. Funct. Mater.* **2014**, *24*, 4090.
- [50] G. Zhu, J. Chen, T. Zhang, Q. Jing, Z. L. Wang, *Nat. Commun.* **2014**, *5*, 3426.
- [51] Y. Zi, S. Niu, J. Wang, Z. Wen, W. Tang, Z. L. Wang, *Nat. Commun.* **2015**, *6*, 8076.
- [52] Q. Jing, Y. Xie, G. Zhu, R. P. Han, Z. L. Wang, *Nat. Commun.* **2015**, *6*, 8031.
- [53] Z. L. Wang, *ACS Nano* **2013**, *7*, 9533.
- [54] Y. Chen, X. Mu, T. Wang, W. Ren, Y. Yang, Z. L. Wang, C. Sun, A. Y. Gu, *Sci. Rep.* **2016**, *6*, 35180.
- [55] J. Wang, S. Li, F. Yi, Y. Zi, J. Lin, X. Wang, Y. Xu, Z. L. Wang, *Nat. Commun.* **2016**, *7*, 12744.
- [56] J. Bae, J. Lee, S. Kim, J. Ha, B.-S. Lee, Y. Park, C. Choong, J.-B. Kim, Z. L. Wang, H.-Y. Kim, *Nat. Commun.* **2014**, *5*, 4929.
- [57] M.-L. Seol, J.-H. Woo, S.-B. Jeon, D. Kim, S.-J. Park, J. Hur, Y.-K. Choi, *Nano Energy* **2015**, *14*, 201.
- [58] L. Zhang, B. Zhang, J. Chen, L. Jin, W. Deng, J. Tang, H. Zhang, H. Pan, M. Zhu, W. Yang, *Adv. Mater.* **2016**, *28*, 1650.
- [59] K. Zhao, Z. L. Wang, Y. Yang, *ACS Nano* **2016**, *10*, 9044.
- [60] S. Li, S. Wang, Y. Zi, Z. Wen, L. Lin, G. Zhang, Z. L. Wang, *ACS Nano* **2015**, *9*, 7479.
- [61] Y. Xie, S. Wang, L. Lin, Q. Jing, Z.-H. Lin, S. Niu, Z. Wu, Z. L. Wang, *ACS Nano* **2013**, *7*, 7119.
- [62] Z. Zhao, X. Pu, C. Du, L. Li, C. Jiang, W. Hu, Z. L. F. Wang, *ACS Nano* **2016**, *10*, 1780.
- [63] S. Wang, X. Mu, X. Wang, A. Y. Gu, Z. L. Wang, Y. Yang, *ACS Nano* **2015**, *9*, 9554.
- [64] X. S. Meng, G. Zhu, Z. L. Wang, *ACS Appl. Mater. Interfaces* **2014**, *6*, 8011.
- [65] S. Wang, Z. L. Wang, Y. Yang, *Adv. Mater.* **2016**, *28*, 2881.
- [66] H. Yong, J. Chung, D. Choi, D. Jung, M. Cho, S. Lee, *Sci. Rep.* **2016**, *6*, 33977.
- [67] M. Taghavi, A. Sadeghi, B. Mazzolai, L. Beccai, V. Mattoli, *Appl. Surf. Sci.* **2014**, *323*, 82.
- [68] S. Gong, W. Schwalb, Y. Wang, Y. Chen, Y. Tang, J. Si, B. Shirinzadeh, W. Cheng, *Nat. Commun.* **2014**, *5*, 3132.
- [69] S. Niu, X. Wang, F. Yi, Y. S. Zhou, Z. L. Wang, *Nat. Commun.* **2015**, *6*, 8975.
- [70] Y. Zi, J. Wang, S. Wang, S. Li, Z. Wen, H. Guo, Z. L. Wang, *Nat. Commun.* **2016**, *7*, 10987.
- [71] T. Q. Trung, N. E. Lee, *Adv. Mater.* **2016**, *28*, 4338.
- [72] H. Zhang, J. Wang, Y. Xie, G. Yao, Z. Yan, L. Huang, S. Chen, T. Pan, L. Wang, Y. Su, *ACS Appl. Mater. Interfaces* **2016**, *8*, 32649.
- [73] Y. Hu, J. Yang, Q. Jing, S. Niu, W. Wu, Z. L. Wang, *ACS Nano* **2013**, *7*, 10424.
- [74] X. Fan, J. Chen, J. Yang, P. Bai, Z. Li, Z. L. Wang, *ACS Nano* **2015**, *9*, 4236.
- [75] J. Yang, J. Chen, Y. Liu, W. Yang, Y. Su, Z. L. Wang, *ACS Nano* **2014**, *8*, 2649.
- [76] J. Wang, C. Wu, Y. Dai, Z. Zhao, A. Wang, T. Zhang, Z. L. Wang, *Nat. Commun.* **2017**, *8*, 88.
- [77] M.-L. Seol, J.-W. Han, D.-I. Moon, M. Meyyappan, *Nano Energy* **2017**, *39*, 238.
- [78] Q. Zheng, Y. Jin, Z. Liu, H. Ouyang, H. Li, B. Shi, W. Jiang, H. Zhang, Z. Li, Z. L. Wang, *ACS Appl. Mater. Interfaces* **2016**, *8*, 26697.
- [79] K. N. Kim, J. Chun, J. W. Kim, K. Y. Lee, J.-U. Park, S.-W. Kim, Z. L. Wang, J. M. Baik, *ACS Nano* **2015**, *9*, 6394.
- [80] Y. Wu, X. Zhong, X. Wang, Y. Yang, Z. L. Wang, *Nano Res.* **2014**, *7*, 1631.
- [81] Z. Quan, C. B. Han, T. Jiang, Z. L. Wang, *Adv. Energy Mater.* **2016**, *6*, 1501799.